Chinese Chemical Letters 33 (2022) 4395–4399

Contents lists available at ScienceDirect

Chinese Chemical Letters

journal homepage: www.elsevier.com/locate/cclet

Two transition-metal-modified Nb/W mixed-addendum polyoxometalates for visible-light-mediated aerobic benzylic C–H oxidations

Yubin Ma[a,1], Fan Gao[b,1], Wanru Xiao[a], Na Li[a], Shujun Li[a,*], Bing Yu[b,*], Xuenian Chen[a,b,*]

[a] School of Chemistry and Chemical Engineering, Henan Key Laboratory of Boron Chemistry and Advanced Energy Materials, Henan Normal University, Xinxiang 453007, China
[b] College of Chemistry, Zhengzhou University, Zhengzhou 450001, China

ARTICLE INFO

Article history:
Received 14 November 2021
Revised 5 December 2021
Accepted 10 December 2021
Available online 17 December 2021

Keywords:
Polyoxometalates
Mixed-addendum POMs
Visible-light-induced catalysis
Photocatalysis
C–H bonds oxidation

ABSTRACT

The visible-light-induced selective oxidation of ubiquitous C–H bonds into valuable C=O bonds under aerobic conditions is one of the most attractive approaches for the construction of carbonyl-containing molecules. In this work, two transition metal-containing Nb/W mixed-addendum POMs dimers with the formula of $K_2Na_2H_5[(Fe(H_2O)_4)_3(P_2W_{15}Nb_3O_{62})_2]\cdot 24H_2O$ (POM[Fe]) and $K_2Na_3H_4[(Cr(H_2O)_4)_3(P_2W_{15}Nb_3O_{62})_2]\cdot 32H_2O$ (POM[Cr]) have been synthesized and characterized by various analytical and spectral techniques. POM[Fe] was proved to be an efficient photocatalyst for benzylic C–H oxidation under visible light and using oxygen as an oxidant to produce the corresponding carbonyl complex in good yields. A plausible mechanism involving superoxide radical was proposed for the catalytic reaction. POM[Fe] showed good reusability in the recycling experiments. IR spectroscopy and XRD analysis indicate that POM[Fe] can retain its integrity after catalysis.

The selective oxidation of benzyl C–H is of significance in modern organic synthesis and pharmaceutical industries [1,2]. Conventionally, benzylic oxidation reactions require not only harsh reaction conditions, but also environmentally unfriendly high-valent oxidants (such as CrO_3, MnO_2 or hypervalent iodine) [3–5]. Therefore, the establishment of a green oxidative system for the benzylic oxidation with oxygen as the mild oxidant is highly attractive. In the past decades, many efforts have been directed toward the development of more efficient catalysts and catalytic systems. For example, a range of transition metal complexes have been employed as catalysts in benzylic oxidation reactions, including the complexes of copper [6], manganese [7], cobalt [8,9], rhodium [10], iron [11,12] and palladium [13]. However, most of the previously reported systems are homogeneous catalysis, in which the catalysts cannot be recovered and reused thus preventing their further application. It is of great significance to develop a recyclable heterogeneous catalyst for the oxidation of benzyl C–H bonds by molecular oxygen under mild and green conditions.

The photocatalytic oxidation of benzyl C–H using visible light is a benign alternative to the classical oxidation method from the perspective of green chemistry and sustainable development [14,15]. Among various photocatalysts, polyoxometalates (POMs) have been proved to be one of the most promising candidates [16–18]. POMs are a large family of metal-oxygen clusters formed by early transition metal with d^0 electronic configuration (M = Mo^{6+}, W^{6+}, Nb^{5+}, Ta^{5+}) [19–24]. Owing to their advantages of diverse and definite structures, adjustable elemental composition and band gap, reversible multielectron processes during catalysis, and high stability toward redox conditions, POMs are attracting more and more attention in the field of photocatalysis [25–28]. They have shown potential applications in photocatalytic degradation of organic pollutants and dyes [29–31], H_2 evolution [32–36] and CO_2 reduction [37–40].

POMs can effectively activate molecular oxygen under light, thereby they can catalyze a variety of organic reactions, such as oxidation of benzene to phenol [41], selective oxidation of alcohols [42], oxidative bromination of arenes and alkenes [43] and coupling reaction of benzylamine [44]. However, in most of these reports, the POMs photocatalysts require UV light. Considering the effective use of solar energy, the development of visible-light-responsive photocatalysts, especially the exploration of their application in some new reactions, are highly demanded.

* Corresponding authors.
E-mail addresses: lisj@htu.edu.cn (S. Li), bingyu@zzu.edu.cn (B. Yu), xnchen@htu.edu.cn (X. Chen).
[1] These authors contributed equally to this work.

https://doi.org/10.1016/j.cclet.2021.12.023
1001-8417/

Herein, we obtained two POMs dimers $K_2Na_2H_5[(Fe(H_2O)_4)_3(P_2W_{15}Nb_3O_{62})_2]\cdot 24H_2O$ (POM[Fe]) and $K_2Na_3H_4[(Cr(H_2O)_4)_3(P_2W_{15}Nb_3O_{62})_2]\cdot 32H_2O$ (POM[Cr]) by the reactions of Nb/W mixed-addenda POM and transition metal (TM) ions (Fe^{3+} and Cr^{3+}) under conventional aqueous solution. The two polyanions both display dimer structures, which are composed of two $\{P_2W_{15}Nb_3\}$ linked by three octahedrally coordinated metal ions. POM[Fe] was proved to be a highly efficient heterogeneous photocatalyst for the visible-light-induced oxidation of benzyl C–H using oxygen as the oxidant. Moreover, the POM[Fe] catalyst displayed excellent cyclability in the catalytic process.

POM[Fe] and POM[Cr] were synthesized in conventional aqueous solution using a Nb/W mixed-addendum precursor $(K_8H[P_2W_{15}(NbO_2)_3O_{59}]\cdot 12H_2O)$ and corresponding transition metal salts ($FeCl_3\cdot 6H_2O$ and $Cr(NO_3)_3\cdot 9H_2O$). The pH values and the use of 2-aminopyrimidine-5-boronic acid pinacol ester play essential roles in the synthesis of the two compounds. The syntheses of the two compounds are performed at different pH values which should be controlled carefully, and upon deviating from the pH ranges, no target product can be afforded. In addition, 2-aminopyrimidine-5-boronic acid pinacol ester served as an essential addition agent, although it does not appear in the final structures of POM[Fe] and POM[Cr]. Only some unidentifiable brownish-yellow precipitates can be obtained without the addition of 2-aminopyrimidine-5-boronic acid pinacol ester at last.

Single-crystal X-ray diffraction structural analysis (Table S1 in Supporting information) reveals that both the two compounds crystallize in space group *P*-1. They exhibit similar structures with only differences in the TM ions. Similar to other transition-metal or rare-earth modified Nb/W mixed-addendum POMs [45–47], the clusters $\{P_2W_{15}Nb_3O_{62}\}$ coordinate with Fe and Cr using the Lewis base terminal O atoms bonded with Nb (O_t(Nb)). Taking POM[Fe] as an example, it consists of two $\{P_2W_{15}Nb_3O_{62}\}$ linked by three $\{FeO_4\}$ to form a sandwich dimer structure (Fig. 1a and Fig. S1 in Supporting information). The three Fe^{3+} ions connect to six O_t(Nb) from two $\{P_2W_{15}Nb_3O_{62}\}$ through three (Nb)O_t-Fe-O_t(Nb) bridges. The Fe-O bond lengths are between 1.920 and 1.943 Å. Each Fe ion adopts six-coordinated octahedral geometry with two O_t(Nb) from POMs and four terminal O atoms (Fig. S1). Bond valence sums (BVS) analyses reveal that the bond valences for all

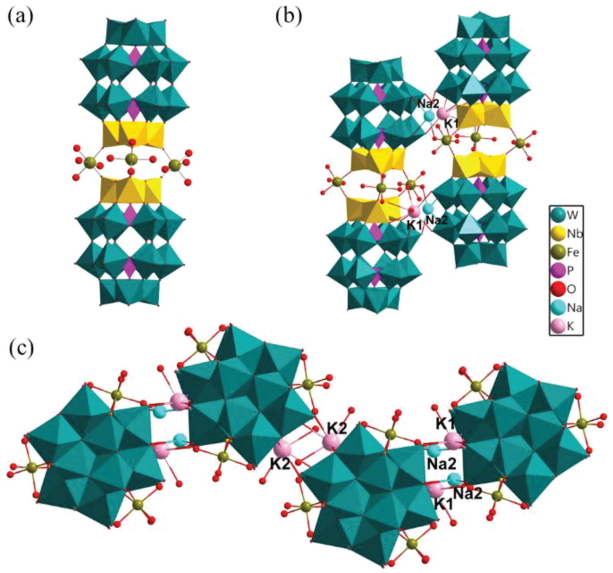

Fig. 1. (a) The polyhedral representation of $[Fe_3(P_2W_{15}Nb_3)_2]$ of POM [Fe]. (b) The polyhedral/ball-and-stick representation of $\{(P_2W_{15}Nb_3O_{62})_4(Fe_3O_{12})_2\}$. (c) Z-shaped one-dimensional (1-D) chain structure of POM[Fe] (top view).

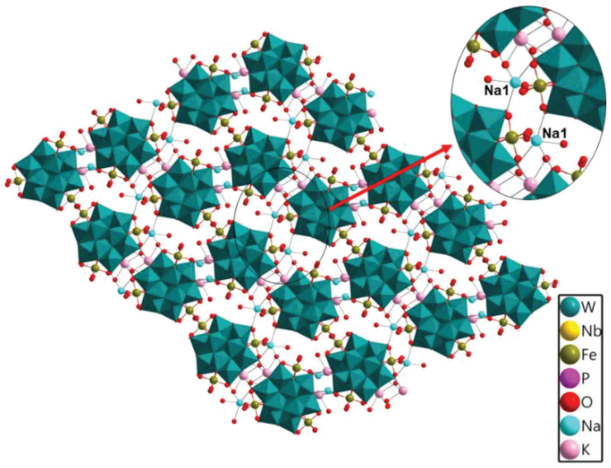

Fig. 2. The 2-D network in POM[Fe] constructed by the building block $\{(P_2W_{15}Nb_3O_{62})_4(Fe_3O_{12})_2\}$ and Na1.

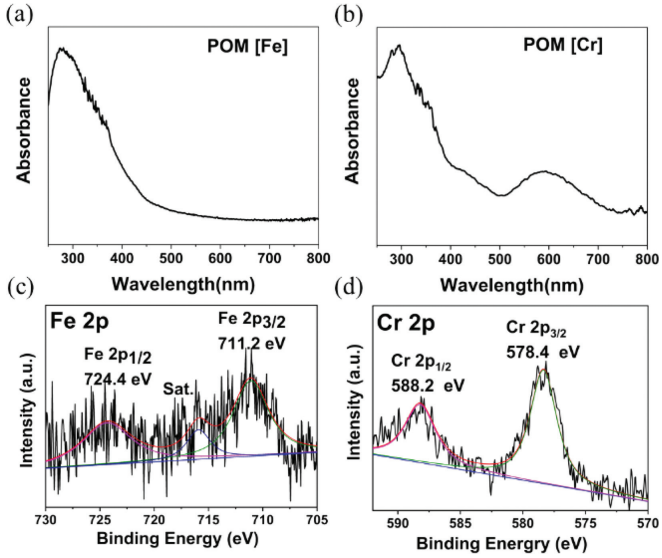

Fig. 3. (a, b) UV-vis spectra and (c, d) XPS spectra for POM[Fe] and POM[Cr].

the four terminal O atoms coordinated with Fe^{3+} are in the range of 0.429 and 0.506 (Table S2 in Supporting information), indicating that all of them exist in the form of coordination water. Two dimeric structures are connected by K1 and Na2 to form a tetrameric $\{(P_2W_{15}Nb_3O_{62})_4(Fe_3O_{12})_2\}$ cluster (Fig. 1b), which are further linked by two additional K ions (K2) to form Z-shaped one-dimensional (1-D) chains (Fig. 1c and Fig. S3 in Supporting information). These 1-D chains are interconnected with each other via Na1 ions resulting in the 2-D networks (Fig. 2).

The character of light absorption of two compounds was investigated by UV-vis diffuse reflection spectroscopy. Due to the presence of transition metals, the UV-vis spectra of POM[Fe] and POM[Cr] exhibit absorption peaks in the visible light region, indicating their potential application in photocatalysis (Figs. 3a and b). The XPS technique was further employed to determine the chemical states of Fe and Cr in POM[Fe] and POM[Cr]. The peaks with binding energies at 724.4 eV and 711.2 eV of POM[Fe] correspond to Fe^{3+} $2p_{1/2}$ and Fe^{3+} $2p_{3/2}$ states, respectively (Fig. 3c) [48,49]. The spectrum of POM[Cr] shows two binding energies at 588.2 eV and 578.4 eV which represent the electrons in the $Cr^{3+}2p_{1/2}$ and Cr^{3+} $2p_{3/2}$ states, respectively (Fig. 3d) [50,51]. The +3 oxidation states of these metal ions indicated by XPS were fully consistent

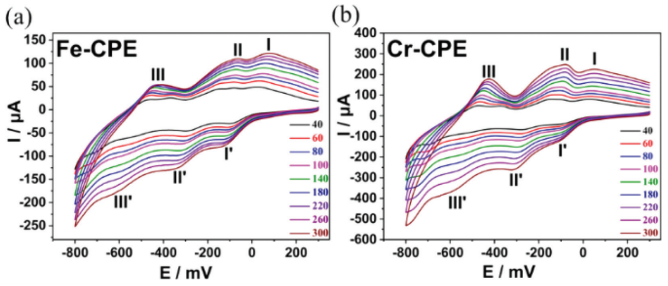

Fig. 4. Cyclic voltammograms of (a) Fe-CPE and (b) Cr-CPE in an aqueous solution of 0.05 mol/L KCl and 0.026 mol/L HCl under different scan rates from inner to outer of 40, 60, 80, 100, 140, 180, 220, 260, 300 mV/s.

with the results of BVS analyses (Table S3 in Supporting information).

To elucidate the electrochemical features of the POM[Fe] and POM[Cr], Fe-CPE and Cr-CPE were prepared for cyclic voltammogram measurements [52]. As shown in Fig. 4, in the potential range of +200 mV to −800 mV, three pairs of redox peaks (I-I', II−II', III−III') are both observed for the two compounds. The two pairs of redox peaks in the negative region of potential values with $E_{1/2}$ peak potentials located at −205 mV (II/II') and −525 mV (III/III') for POM[Fe] and −195 mV (II/II') and −550 mV (III/III')) for POM[Cr] are assigned to the redox process of the W centers [53]. A couple of redox peaks in the region with an $E_{1/2}$ peak potential of −20 mV (I/I') for POM[Fe] and −25 mV (I/I') for POM[Cr] are attributed to the Fe and Cr centers, respectively [54]. Their peak currents were proportional to the square root of the scan rates, which indicates that their redox processes are both diffusion-controlled (Fig. S4 in Supporting information).

To gain the optimization for the reaction conditions, a series of experiments were conducted by using isochromane (**1a**) as the model substrate to examine the catalytic activity of POM[Cr] and POM[Fe] under irradiation of visible light at room temperature (Table 1). Initially, different wavelengths including 390, 430, 460, 520 nm (green light), and white light were examined for the model reaction in CH_3CN at room temperature till full conversation, monitoring by thin-layer chromatography (TLC) (entries 1–5). These results revealed that 390 nm was the best light source, leading to the desired product **2a** in moderate isolated yield (68%, entry 1). However, considering the significance of visible light in organic synthesis and the negligibly different yields between 390 and 430 nm (entries 1 and 2), we decided to use 430 nm as the optimized light source for further study. When POM[Cr] was employed as photocatalyst in the model reaction, a lower yield of desired product **2a** was obtained (entry 6). To further improve the reaction efficiency, a series of solvents including dimethyl sulfoxide (DMSO), H_2O, EtOH, dimethyl carbonate (DMC), 1,2-dichloroethane (DCE), acetone, *N,N*-dimethylformamide (DMF), toluene, 1-butyl-3-methylimidazolium tetrafluoroborate ([BMIM]BF_4) and 1,4-dioxane were screened (entries 7–16). The results showed that when DMSO, H_2O, and acetone were employed as a solvent the yields of **2a** were 72%, 71% and 71%, respectively (entries 7, 8 and 12). Given that the catalyst POM[Fe] is soluble in water while insoluble in acetone, we choose acetone as the optimal reaction solvent making POM[Fe] a heterogeneous catalyst. Finally, the examination of the amount of catalyst showed that 0.5 mol% of catalyst was the best amount for this transformation (entries 17–20). Therefore, the optimal conditions were established as follows: **1a** (0.4 mmol) and photocatalyst POM[Fe] (0.5 mol%) in acetone (0.2 mol/L) were stirred at room temperature under the irradiation of blue light (430 nm) with O_2 (1 atm) as the sole oxidant.

With the optimized conditions in hand, the generality and limitation of this photocatalytic oxygenation protocol were evaluated by examining diverse compounds (Scheme 1). Firstly, different oxygen-containing heterocycles could be oxidized to corresponding lactones **2a** and **2b** or ketone **2c** in moderate to good yields (43%−76%). 2,3-Dihydro-1*H*-indene and 1,2,3,4-tetrahydronaphthalene afforded the desired product **2d** and **2e** with the yield of 68% and 63%, respectively. Then, the aromatic substrates with more active methylene could be easily oxidized to generate ketones **2f-2i** (46%–82%). Especially, 9,10-dihydroanthracene **1f** gave the corresponding anthracene-9,10-dione **2f** in the yield of 58%. Encouraged by these results, diverse functional groups (–H, $–CH_3$, –OMe, $–CH_2Ph$, –Ph, –Py) on the benzylic position were further evaluated. It was found that all of the compounds **1j-1o** could be oxidized under the optimized reaction conditions albeit with a longer reaction time (**2j-2o**). Finally, *N*-heterocyclic compounds were further evaluated in this photocatalytic system, generating the corresponding products **2p-2s** in moderated yields (43%−61%). It is a pity that this protocol failed to realize the selective mono-oxidation of isoindoline **1s**, which has great value in medicines and materials [55]. Moreover, we also found that the current catalytic system has some limitations. For example, the *N*-heterocyclic compounds **1t-1y** and the aliphatic substrate **1z** are not suitable in this oxidative reaction.

To get a deep insight into the reaction mechanism, a series of control experiments were conducted as shown in Table 2. Firstly, we concluded that oxygen was an essential and efficient factor *via* carrying out reaction under air and nitrogen atmosphere (Table 2, entries 2 and 3). Then, no desired product was obtained without light irradiation, indicating that light is of significance in this process (Table 2, entry 4). Radical scavengers (2,2,6,6-

Table 1
Optimization of the reaction.[a]

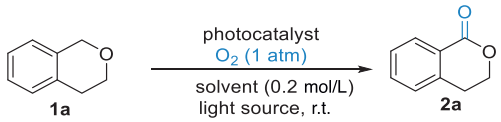

Entry	Photocatalyst (0.25 mol%)	Light source (10 W)	Solvent (0.2 mol/L)	Yield (%)[b]
1	POM[Fe]	390 nm	CH_3CN	68
2	POM[Fe]	430 nm	CH_3CN	65
3	POM[Fe]	460 nm	CH_3CN	52
4	POM[Fe]	green	CH_3CN	trace
5	POM[Fe]	white	CH_3CN	21
6	POM[Cr]	430 nm	CH_3CN	45
7	POM[Fe]	430 nm	DMSO	72
8	POM[Fe]	430 nm	H_2O	71
9	POM[Fe]	430 nm	EtOH	62
10	POM[Fe]	430 nm	DMC	43
11	POM[Fe]	430 nm	DCE	67
12	POM[Fe]	430 nm	Acetone	71
13	POM[Fe]	430 nm	DMF	23
14	POM[Fe]	430 nm	Toluene	46
15	POM[Fe]	430 nm	[BMIM]BF_4	15
16	POM[Fe]	430 nm	1,4-Dioxane	48
17[c]	–	430 nm	Acetone	41
18[d]	POM[Fe]	430 nm	Acetone	59
19[e]	POM[Fe]	430 nm	Acetone	76
20[f]	POM[Fe]	430 nm	Acetone	54

[a] All reactions were performed by using **1a** (0.4 mmol), photocatalyst (0.25 mol%) and solvent (0.2 mol/L) under 10 W blue LED, stirred at room temperature and in O_2 for 24 h. DMSO = dimethyl sulfoxide, DMC = dimethyl carbonate; DCE = 1,2-dichloroethane; DMF = *N,N*-dimethylformamide; [BMIM]BF_4 = 1-butyl-3-methylimidazolium tetrafluoroborate.
[b] Isolated yield;
[c] Without photocatalyst;
[d] Photocatalyst (0.125 mol%);
[e] Photocatalyst (0.5 mol%);
[f] Photocatalyst (1 mol%).

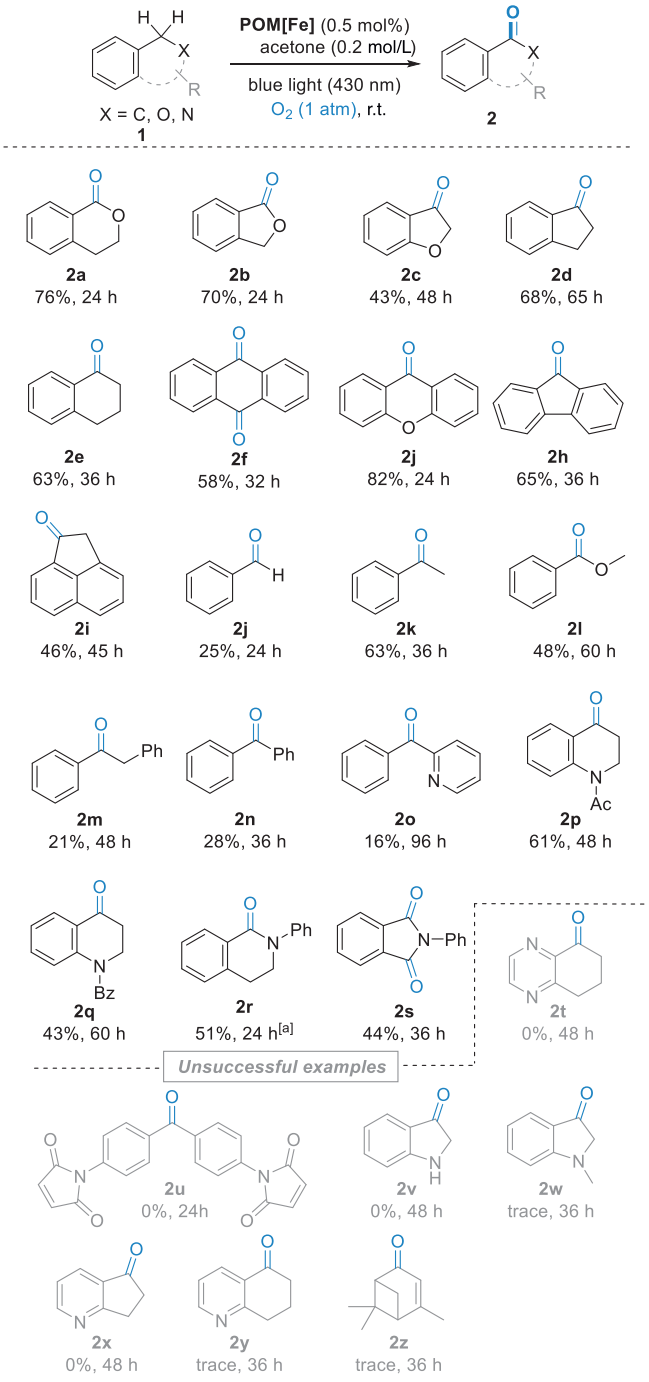

Scheme 1. Substrate scope. Reaction conditions: **1** (0.4 mmol), POM[Fe] (0.5 mol%), acetone (0.2 mol/L), blue LED (430 nm, 10 W), using O_2 balloon at room temperature. Isolated yields were given. [a] EtOH instead of acetone.

tetramethylpiperidin-1-yl)oxidanyl (TEMPO) was added under standard conditions (Table 2, entry 5). This reaction was inhibited, indicating that a radical mechanism may be involved in this protocol. Meanwhile, the adduct of TEMPO and radical species from **1a** (*i.e.*, intermediate **3** in Scheme 2) was detected by using high-resolution mass spectroscopy (HRMS) (Fig. S8 in Supporting information). Additionally, when superoxide radical scavenger 4-benzoquinone (BQ) [56] was added into the reaction, the decreased yield of **2a** demonstrated that superoxide radical was generated and played an important role in the reaction process (Table 2, entry 6). Finally, hydroperoxide radical may exist in this system through the result of adding $FeSO_4$ under standard conditions (Table 2, entry 7).

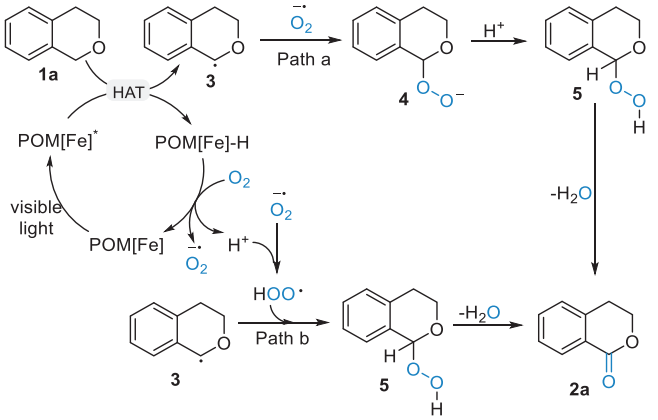

Scheme 2. Plausible reaction mechanism.

Table 2
Control experiments.[a]

Entry	Varied condition	Yield (%)	Conclusions
1	None	76	None
2	Air instead of O_2	68	Efficient
3	N_2 instead of O_2	0	Essential
4	Without light	trace	Essential
5	Added 4 equiv. of TEMPO	0	Radical
6	Added 2 equiv. of BQ	16	Peroxide radical
7	Added 2 equiv. of $FeSO_4$	57	Hydroperoxide radical

[a] Standard conditions: **1a** (0.4 mmol), POM[Fe] (0.5 mol%), acetone (0.2 mol/L), 10 W blue LED (430 nm), using O_2 balloon at room temperature for 24 h. Isolated yields were given.

Based on the above experimental results, a plausible mechanism was proposed as shown in Scheme 2. Firstly, ground state POM[Fe] was transformed into excited state POM[Fe]* under the irradiation of visible light. Then, substrate **1a** underwent a hydrogen atom transfer (HAT) process under the effect of excited state POM[Fe]* to generate intermediate **3**, along with the generation of POM[Fe]-H. Intermediate POM[Fe]-H was oxidized by oxygen to regenerate the ground state POM[Fe] to accomplish the photoredox cycle and release a proton. Simultaneously, oxygen was transformed into a superoxide radical. On the one hand, intermediate **3** was combined with superoxide radical to generate intermediate **4**, which was protonated to obtain intermediate **5** (path a). On the other hand, intermediate **3** reacted with hydroperoxide radical to generate intermediate **5** (path b). Finally, intermediate **5** released H_2O to afford desired products **2a**.

The stability and reusability of POM[Fe] were also evaluated. After the reaction, photocatalyst POM[Fe] was isolated by centrifugation, washed with 15 mL CH_2Cl_2 three times, and air-dried at room temperature for 24 h, then directly used in the next reaction. As shown in Fig. 5, good stability and high catalytic activity of POM[Fe] was demonstrated due to the negligibly decreased yield of **2a** after the 7th cycle. Meanwhile, the results of PXRD patterns and FTIR spectroscopy of recovered POM[Fe] also indicated the good stability and well-maintained in crystal lattice (Fig. S9 in Supporting information).

In summary, two POM dimers have been successfully synthesized by the reaction of Nb/W mixed-addendum POM and TM ions (Fe^{3+} and Cr^{3+}). POM[Fe] can efficiently catalyze the selective oxidation of sp^3 C–H bonds under visible light using oxygen as an

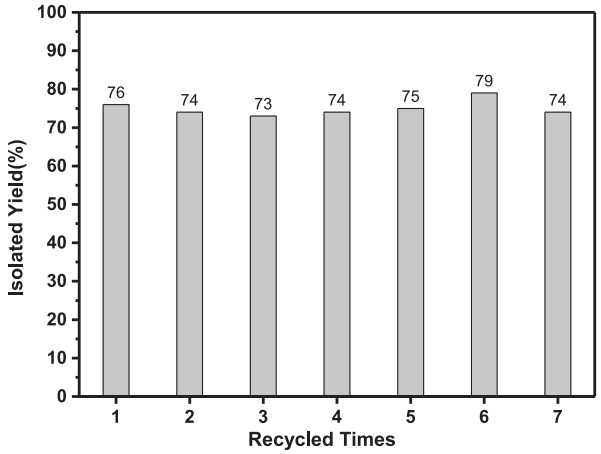

Fig. 5. Recycling experiments.

oxidant. The catalyst shows good stability and reusability in multiple catalytic cycles. Mechanistic investigations suggest that the catalytic reaction has gone through a hydrogen atom transfer process. The superoxide radical has generated and played an important role in the reaction processes. This work provides a feasible revelation for exploring the development of new transition metal-modified POMs in visible-light-induced organic reactions.

Declaration of competing interest

The authors declare that they have no known competing financial interests or personal relationships that could have appeared to influence the work reported in this paper.

Acknowledgments

This work was supported by the National Natural Science Foundation of China (Nos. 22171073, 21971224 and U1804253), and the Natural Science Foundation of Henan Province (No. 202300410246).

Supplementary materials

Supplementary material associated with this article can be found, in the online version, at doi:10.1016/j.cclet.2021.12.023.

References

[1] L. Kesavan, R. Tiruvalam, M.H.A. Rahim, et al., Science 331 (2011) 195–199.
[2] H. Sterckx, B. Morel, B.U.W. Maes, Angew. Chem. Int. Ed. 58 (2019) 7946–7970.
[3] J. Muzart, Chem. Rev. 92 (1992) 113–140.
[4] W.W.Y. Lam, S.M. Yiu, J.M.N. Lee, et al., J. Am. Chem. Soc. 128 (2006) 2851–2858.
[5] S. Yamazaki, Org. Lett. 1 (1999) 2129–2132.
[6] J. Liu, X. Zhang, H. Yi, et al., Angew. Chem. Int. Ed. 54 (2015) 1261–1265.
[7] G. Olivo, G. Farinelli, A. Barbieri, et al., Angew. Chem. Int. Ed. 56 (2017) 16347–16351.
[8] N. Sauermann, T.H. Meyer, C. Tian, et al., J. Am. Chem. Soc. 139 (2017) 18452–18455.
[9] D.P. Hruszkewycz, K.C. Miles, O.R. Thiel, et al., Chem. Sci. 8 (2017) 1282–1287.
[10] Y. Wang, Y. Kuang, Y. Wang, Chem. Commun. 51 (2015) 5852–5855.
[11] B. Mühldorf, R. Wolf, Angew. Chem. Int. Ed. 55 (2016) 427–430.
[12] P.E. Gormisky, M.C. White, J. Am. Chem. Soc. 135 (2013) 14052–14055.
[13] L.V. Desai, K.L. Hull, M.S. Sanford, J. Am. Chem. Soc. 126 (2004) 9542–9543.
[14] H. Yi, C. Bian, X. Hu, et al., Chem. Commun. 51 (2015) 14046–14049.
[15] L. Ren, M.M. Yang, C.H. Tung, et al., ACS Catal. 7 (2017) 8134–8138.
[16] S.S. Wang, G.Y. Yang, Chem. Rev. 115 (2015) 4893–4962.
[17] K. Suzuki, N. Mizuno, K. Yamaguchi, ACS Catal. 8 (2018) 10809–10825.
[18] C. Streb, K. Kastner, J. Tucher, Phys. Sci. Rev. 4 (2019) 20170177.
[19] M.T. Pope, A. Müller, Angew. Chem. Inter. Ed. 30 (1991) 34–48.
[20] D.L. Long, R. Tsunashima, L. Cronin, Angew. Chem. Int. Ed. 49 (2010) 1736–1758.
[21] M. Nyman, F. Bonhomme, T.M. Alam, et al., Science 297 (2002) 996–998.
[22] G. Yang, X. Zhang, Y. Liu, et al., Inorg. Chem. Front. 8 (2021) 4650–4656.
[23] G. Yang, K. Li, X. Lin, et al., Chin. J. Chem. 39 (2021) 3017–3022.
[24] M. Lv, Y. Liu, K. Li, et al., Tetrahedron Lett. 65 (2021) 152757.
[25] A. Hiskia, A. Mylonas, E. Papaconstantinou, Chem. Soc. Rev. 30 (2001) 62–69.
[26] T. Yamase, Chem. Rev. 98 (1998) 307–326.
[27] C. Streb, Dalton Trans. 41 (2012) 1651–1659.
[28] L. Yang, J. Lei, J.M. Fan, et al., Adv. Mater. 33 (2021) 2005019.
[29] R. Dehghani, S. Aber, F. Mahdizadeh, Clean Soil Air Water 46 (2018) 1800413.
[30] J. Lan, Y. Wang, B. Huang, et al., Nanoscale Adv. 3 (2021) 4646–4658.
[31] S.Y. Lai, K.H. Ng, C.K. Cheng, et al., Chemosphere 263 (2021) 128244.
[32] M. Zhang, H. Li, J. Zhang, et al., Chin. J. Catal. 42 (2021) 855–871.
[33] S. Li, S. Liu, S. Liu, et al., J. Am. Chem. Soc. 134 (2012) 19716–19721.
[34] X.J. Kong, Z. Lin, Z.M. Zhang, et al., Angew. Chem. Int. Ed. 55 (2016) 6411–6416.
[35] Z. Zhang, Q. Lin, D. Kurunthu, et al., J. Am. Chem. Soc. 133 (2011) 6934–6937.
[36] Y. Luo, S. Maloul, M. Wächtler, et al., Chem. Commun. 56 (2020) 10485–10488.
[37] J. Gu, W. Chen, G.G. Shan, et al., Mater. Today Energy 21 (2021) 100760.
[38] J. Ettedgui, Y. Diskin-Posner, L. Weiner, et al., J. Am. Chem. Soc. 133 (2011) 188–190.
[39] S.-L. Xie, J. Liu, L.Z. Dong, et al., Chem. Sci. 10 (2019) 185–190.
[40] S. Barman, S.S. Sreejith, S. Garai, et al., ChemPhotoChem 3 (2019) 93–100.
[41] Y. Gu, Q. Li, D. Zang, et al., Angew. Chem. Int. Ed. 60 (2021) 13310–13316.
[42] M. Bonchio, M. Carraro, G. Scorrano, et al., Adv. Synth. Catal. 345 (2003) 1119–1126.
[43] A. Molinari, G. Varani, E. Polo, et al., J. Mol. Catal. A: Chem. 262 (2007) 156–163.
[44] S. Li, G. Li, P. Ji, et al., ACS Appl. Mater. Interfaces 11 (2019) 43287–43293.
[45] D. Zhang, J. Luo, Y. Ma, et al., Inorg. Chem. 59 (2020) 6747–6754.
[46] S.J. Li, S.X. Liu, N.N. Ma, et al., CrystEngComm 14 (2012) 1397–1404.
[47] W. Xiao, S. Li, Y. Zhao, et al., Dalton Trans. 50 (2021) 8690–8695.
[48] I. Chakraborty, P. Baran, Y. Sanakis, et al., Inorg. Chem. 47 (2008) 11734–11737.
[49] H.H. Wu, Z.M. Zhang, E.B. Wang, Chin. Chem. Lett. 23 (2012) 355–358.
[50] J. Wang, S. Atif, D. Zhang, Environ. Technol. Innov. 20 (2020) 101088.
[51] V. Singh, J. Singh, V. Mishra, J. Environ. Chem. Eng. 9 (2021) 105124.
[52] P. Zhang, J. Peng, X. Shen, et al., J. Solid. State. Chem. 182 (2009) 3399–3405.
[53] N. Zhang, L. Hong, A. Geng, et al., Chin. Chem. Lett. 29 (2018) 1409–1412.
[54] I.M. Mbomekalle, B. Keita, L. Nadjo, et al., Inorg. Chem. 42 (2003) 1163–1169.
[55] S. Das, D. Addis, L.R. Knöpke, et al., Angew. Chem. Int. Ed. 50 (2011) 9180–9184.
[56] S. Yang, S. Zhu, D. Lu, et al., Org. Lett. 21 (2019) 2019–2024.